

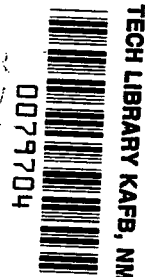
NASA TECHNICAL NOTE



NASA TN D-2730

NASA TN D-2730

LOAN COPY: R
AFWL (W
KIRTLAND AF



COMPARISON OF MEASURED AND CALCULATED SONIC-BOOM GROUND PATTERNS DUE TO SEVERAL DIFFERENT AIRCRAFT MANEUVERS

by Donald L. Lansing and Domenic J. Maglieri

Langley Research Center

Langley Station, Hampton, Va.



COMPARISON OF MEASURED AND CALCULATED
SONIC-BOOM GROUND PATTERNS DUE TO SEVERAL
DIFFERENT AIRCRAFT MANEUVERS

By Donald L. Lansing and Domenic J. Maglieri

Langley Research Center
Langley Station, Hampton, Va.

NATIONAL AERONAUTICS AND SPACE ADMINISTRATION

For sale by the Office of Technical Services, Department of Commerce,
Washington, D.C. 20230 -- Price \$2.00

COMPARISON OF MEASURED AND CALCULATED
SONIC-BOOM GROUND PATTERNS DUE TO SEVERAL
DIFFERENT AIRCRAFT MANEUVERS

By Donald L. Lansing and Domenic J. Maglieri
Langley Research Center

SUMMARY

Detailed comparisons of the measured and calculated ground shock pressure patterns resulting from aircraft performing pushover-dive-pullout, longitudinal-acceleration, pullup-climb-pushover, and circular-turn maneuvers are presented. Calculation of the arrival time of the shock wave and the pressure amplitude as a function of distance along the ground are compared with the measurements from an array of microphones. Specific cases are also presented in which the superboom phenomena were obtained.

The comparison between acoustic theory and experiment which is presented in this paper indicates that the theoretical method used is capable of predicting the essential features of the ground shock patterns of aircraft in maneuvers at altitudes below 30,000 to 40,000 feet at least when the sound speed gradient is nearly linear. In particular, the theory predicts the correct number of N-waves which will occur in the vicinity of a given ground area and gives reasonable estimates of the time elapsed between the generation of the boom and its arrival on the ground. In general, the calculated elapsed times are a few seconds less than those measured. The calculated overpressures either agree well with measurements or give a slight overestimate in those ground areas which do not experience superboom phenomena. The results suggest that the location of superboom phenomena can be predicted to within plus or minus 2 to 3 miles, provided accurate aircraft position information and weather data are available.

INTRODUCTION

The possibility of pressure buildups on the ground due to aircraft accelerations in supersonic flight is of concern in the operation of all types of military and civilian supersonic aircraft. Since at present it does not seem feasible to eliminate such pressure buildups completely, there is much interest in the basic phenomena and in operational procedures that will minimize their effects. In order to devise such operating procedures, it is necessary to have an understanding of the manner in which aircraft operation and the properties of the atmosphere affect the overpressure-distribution pattern on the ground.

Theoretical studies of the effects of maneuvers on the location and strength of sonic booms have been carried out from the standpoint of geometrical acoustics in a number of investigations. (See refs. 1 to 5.) The basic equations governing the acoustic approximation of the shock-wave ground pattern have been put into a form convenient for machine computation in reference 6. Some calculations using this acoustic theory and assuming a linear sound speed gradient have been made in conjunction with a series of flight-test experiments (ref. 7); the main results are reported briefly in reference 8. A more recent theoretical method which allows for a step-by-step adjustment for wind and temperature effects, thus permitting any arbitrary gradients to be included, is formulated in reference 9.

The present paper presents a detailed comparison of the measured ground shock pattern resulting from aircraft performing four specific supersonic maneuvers with the analytical results based on the method given in reference 6. The measurements were obtained during a special series of flights which were performed at altitudes below the tropopause and for which accurate radar-tracking and weather-sounding information were obtained. The specific supersonic maneuvers for which both experimental and analytical data are presented are a pushover-dive-pullout, longitudinal acceleration at constant altitude, pullup-climb-pushover, and a circular turn at constant altitude. Calculations of the elapsed time of the shock waves and pressure amplitudes on the ground are compared with measurements from an array of microphones. In addition, some calculations based on the analytical method presented in reference 9 are compared with the experimental results.

SYMBOLS

a	component of aircraft acceleration toward an observer
c_0	speed of sound at the ground
c	speed of sound
d	maximum diameter of an equivalent body of revolution
g	acceleration due to gravity
K_B	body shape factor
K_R	reflection coefficient
l	aircraft length
m	rate of decrease of speed of sound with altitude, $\frac{dc}{dz}$
M	aircraft Mach number

p_a	ambient pressure at altitude
p_o	ambient pressure at the ground
Δp_o	shock-wave overpressure at ground
s	distance from flight path to observer
t	elapsed time from the time that the aircraft is overhead the x = 0 position until the shock wave arrives at any arbitrary position
z	altitude above ground
γ	ratio of specific heats
$\lambda = \frac{(M^2 - 1)c^2}{a}$	
x	distance along microphone array, measured from center of array, ft

TEST CONDITIONS AND PROCEDURES

The tests were conducted in the vicinity of Edwards Air Force Base, California, during September and October of 1961 as part of a joint NASA-USAF-FAA sonic-boom research program. The measurements were made in the vicinity of Rogers Dry Lake, which was generally flat and open. (See ref. 7.)

The special flights performed for this study were accomplished with a fighter aircraft having a length of 54.5 feet and a gross weight of about 20,000 pounds. A log of these special flights for which calculations have been made is given in table I.

Radar plotting board overlays were obtained for all flights. The radar tracking provided altitude and plan position of the aircraft at 1-second intervals (see fig. 4 of ref. 7). The velocity of the aircraft was obtained by numerically differentiating the position data. In order to synchronize the tracking data with all ground pressure measurements, a 1,000 cps tone signal was superposed on the data records at the time the aircraft passed over the main recording station.

Rawinsonde observations from the Edwards Air Force Base weather facility located about 9 miles from the test area were taken within 3 hours of the times of all test flights. The measured values of temperature, pressure, and wind velocity and direction were provided at 1,000-foot intervals to altitudes in excess of the airplane test altitude. The speed of sound was calculated from these measured data.

Measurements of the ground pressures were accomplished by means of an array of 8 microphones located in a straight line extending about 4 miles. This line was essentially directly beneath the flight path of the aircraft in dive maneuvers and linear accelerations. The response characteristics of this equipment were sufficient to reproduce faithfully the sonic-boom signatures for the various conditions of these tests. The microphones were shock mounted in ground reflecting boards and equipped with wind and sand screens as described in reference 7.

Figure 1 illustrates the manner of accomplishing the flight tests for the case of a longitudinal acceleration. Figure 1(a) illustrates the location of the flight and ground tracks relative to the ground microphone array. Figure 1(b) is a sketch of the shock-wave formations on the ground for a longitudinal-acceleration maneuver. This figure includes a perspective-view sketch of only the bow shock-wave patterns, and, for simplicity, these are shown only on one side of the ground track. It is significant to note that there is a substantial distance between the point on the ground below the aircraft at the Mach 1 condition and the point where the shock first arrives at the ground. It is therefore necessary to start the airplane acceleration at some distance ahead of the location of the ground measurement array in order that the shock-wave pattern (particularly the cusp formations) will impinge in the area in which the instruments are located. It was considered important for the purposes of the studies to record at each measuring station the arrival times of each disturbance. In some cases multiple disturbances occur and these arrive at different times as indicated by the sample pressure traces shown at the bottom of figure 1(b). Although it can be seen from the sketch in figure 1(b) that cusp formations may exist at various lateral distances from the ground track, the measurements of the present investigation were limited to locations on the ground track except for the turn maneuvers.

Figure 2 presents schematic profile and planviews of the four types of maneuvers treated in the present paper. Since a number of flights were usually made for each type of maneuver (see table I), the values of altitude, Mach number, and horizontal distance from the microphone ground array as listed on the figure are only approximate. Figure 2(a) presents a profile view of a longitudinal-acceleration maneuver at constant altitude; figure 2(b), the pushover-dive-pullout maneuver; figure 2(c), the pullup-climb-pushover maneuver; and figure 2(d), the circular-turn maneuver at constant altitude.

METHOD OF CALCULATION

Position and Arrival Time of the Shock Wave on the Ground

The method used for calculating the location of the shock wave on the ground was the ballistic wave method described in detail in reference 6. This method treats the aircraft as a moving point source of acoustic disturbances and computes the position on the ground of the envelope of the wave fronts produced along the flight path. This scheme does not take into account the effect of winds on the propagation of the shock wave and is limited to altitudes below

about 40,000 feet since a linear decrease in the speed of sound with altitude is assumed in determining the shape of the wave fronts.

This method has the advantage that it results in a computation of the ground shock pattern directly without making any intermediate use of ray paths. The ground shock pattern as it appears at any instant of time can be calculated if the previous history of the aircraft position and velocity along its flight path are known. By plotting the ground shock patterns formed at successive instants of time, it is possible to determine when the shock will arrive at a given ground position and the location of the aircraft at that time. It is also possible to determine those portions of the flight path which give rise to such phenomena as cusps, foci, and multiple booms. A physical description of the manner in which the ground patterns are formed and a discussion of the types of ground shock phenomena which may be produced by typical maneuvers are given in reference 6.

The linear variation in the speed of sound used in each computation was obtained by fairing a straight line through plots of speed of sound against altitude calculated from temperature data measured by conventional rawinsonde equipment prior to each test flight. A linear approximation to the speed of sound was adequate for all maneuver flights. The measured speed of sound was generally close to that expected for a standard atmosphere. For several flights, however, the sound speed gradient was considerably less than that in a standard atmosphere.

Figure 3 shows two sample plots of the variation in the speed of sound with altitude as obtained from rawinsonde data and the corresponding linear variation assumed in the calculations. The plots are cut off below 2,500 feet which is approximately the altitude of the test site. In the left-hand plot in figure 3 the measured sound speed gradient below about 15,000 feet is only about 0.0020 ft per sec/ft or roughly half that in a standard atmosphere (≈ 0.0040 ft per sec/ft). For the left-hand plot in figure 3 the maneuvers performed were linear accelerations at about a 14,000-foot altitude. For the right-hand plot in figure 3 for which the sound speed gradient was nearly equal to that of a standard atmosphere, the maneuvers were circular turns at about a 30,000-foot altitude.

Overpressure of Shock Wave on the Ground

Whitham's formula for calculating the volume contribution (lift contribution assumed to be zero) to the strength of the bow shock of an aircraft in level constant-speed flight in a homogeneous atmosphere (ref. 10) was modified by Rao (ref. 2) to take into account the effects of acceleration and flight-path curvature. Rao's formula can be written

$$\frac{\Delta p_o}{p_\infty} = K_B \frac{d}{z^{1/4}} \frac{M^{3/4}}{(M^2 - 1)^{1/4}} \frac{1}{\sqrt{s \left(1 - \frac{s}{\lambda}\right) B(s, \lambda)}} \quad (1)$$

where Δp_0 is the pressure jump across the bow shock, p_∞ is the pressure in the undisturbed air, K_B is the body shape factor, d is the maximum diameter of an equivalent body of revolution, l is the length of the aircraft, and M is the aircraft Mach number. The quantity s is the distance traveled by the shock along a straight line joining the observer to the point on the flight path at which the observed shock originated. This line is a ray in a homogeneous atmosphere. The quantity λ is defined by $\lambda = \frac{(M^2 - 1)c^2}{a}$ where c is the speed of sound in the undisturbed air and a is the component of the aircraft acceleration along the line joining the observer and the flight path. The function $B(s, \lambda)$ is given in reference 2. In particular, for steady-level flight, $a = 0$, $\lambda = \infty$, $B(s, \lambda) = \sqrt{s}$, and the equation reduces to that of Whitham when s is replaced by the perpendicular distance from observer to the flight path.

A modified form of equation (1) was used in this paper to compute the ground shock-wave overpressures for each maneuver flight. The following modifications of the equation were introduced in a rough attempt to take into account the inhomogeneity of the atmosphere. The pressure p_∞ was replaced by $\sqrt{p_a p_0}$ where p_a is the pressure at the altitude where the shock was generated, and p_0 is the pressure at the ground. (See ref. 3.) Similarly c and M were used as the speed of sound and aircraft Mach number at the altitude and time at which the observed shock was generated. The definitions of the quantities s and a remain unchanged. Although the ray joining the observer to the flight path is no longer a straight line, s was used as the straight-line distance for the purposes of the overpressure calculations. Since a linear decrease in the speed of sound with altitude is assumed in computing the location of the ground shock pattern, the rays are arcs of circles. The components of the aircraft acceleration needed in computing a and λ were obtained by numerically differentiating the aircraft velocity components which were obtained from the tracking information. For comparison with experiment, the right-hand side of equation (1) must be multiplied by K_R , the reflection coefficient, to take into account the fact that the microphones were flush mounted in plywood boards at ground level and therefore measured approximately twice the overpressures in free air.

The pressure p_a was calculated from the equation

$$p_a = p_0 \exp\left(-\frac{g\gamma}{c_0} \frac{z}{c_0 - mz}\right)$$

in which z is altitude, p_0 is the pressure at the ground, c_0 is the speed of sound at the ground, m is the rate of decrease of the speed of sound with altitude, g is the acceleration due to gravity, and γ is the ratio of specific heats. This equation is a simplified form of the results presented in reference 11 and was found to represent quite accurately the measured variation of pressure with altitude. The pressure at the ground p_0 was obtained from

rawinsonde data and was essentially constant at 1950 lb/ft², which is approximately the pressure in a standard atmosphere at the altitude of the test site. Rawinsonde data were used in determining values of c_0 and m as described previously.

Combining these results gives the final form of the equation used in calculating the ground overpressures:

$$\Delta p_0 = p_0 K_B K_R \frac{d}{l^{1/4}} \frac{M^{3/4}}{(M^2 - 1)^{1/4}} \frac{\exp\left(-\frac{gy}{2c_0} \frac{z}{c_0 - mz}\right)}{\sqrt{s\left(1 - \frac{s}{\lambda}\right)} B(s, \lambda)}$$

For the calculations presented in this paper $K_R = 2.0$; $K_B = 0.60$; $d = 6.5$ ft; $l = 54.5$ ft; $gy = 45.0$.

EXPERIMENTAL RESULTS AND COMPARISON WITH THEORY

Figures 4 to 8 show a comparison between the calculated and experimental results for the 14 maneuver flights listed in table I. For each maneuver the overpressures Δp_0 at the ground and the elapsed time t (based on an arbitrary reference time) of the bow shock of each complete N-wave which passed over the main microphone array are presented as a function of distance x along the array. (See fig. 2.) The distance x used as the abscissa on the Δp_0 and t plots is measured along the microphone array with the origin ($x = 0$) about in the middle of the array. In a dive or acceleration the aircraft moves in the direction of increasing x , that is, from left to right. (See fig. 2.) The symbolized data points indicate the experimental data and the lines are the theoretical results. The first N-wave to arrive at a microphone usually had the highest overpressure.

For dive and acceleration maneuvers, the elapsed time t is the difference between the time at which the aircraft passed over the center of the microphone array ($x = 0$) and the time of arrival of the shock wave at any microphone position. For the circular-turn maneuvers t was determined in a similar manner except that the reference time $t = 0$ was chosen as the time at which the aircraft passed over point A as indicated in figure 2(d).

The zero reference for determining the elapsed time t was arbitrarily chosen. The resulting values of t are generally smaller than the total transit time required by the shock to travel from its point of origin on the flight path to an observer on the ground. The transit time is a function of observer location, aircraft altitude, Mach number, heading, and atmospheric conditions. For an observer on the flight track and a standard atmosphere, the theoretical range of values of the transit time for the maneuvers presented in this paper are about: 30 to 95 seconds for the pushover-dive-pullout maneuvers; 30 to 80 seconds for the linear accelerations, and 50 to 60 seconds for

the pullup-climb-pushover maneuver. For the circular-turn maneuvers the transit time varies from about 45 seconds for an observer on a ray directly beneath the aircraft to about 120 seconds for an observer on one of the grazing rays. (See ref. 6.)

Because of the arbitrary reference used in presenting the elapsed-time data in figures 4 to 8, it is not possible to determine the accuracy of elapsed-time predictions directly from the figures.

Pushover-Dive-Pullout Maneuver

Figure 4 shows a comparison of the results for four supersonic-pushover-dive-pullout maneuvers. These maneuvers were executed in a vertical plane as illustrated in figure 2(b). For figure 4(a) the minimum altitude was only 10,000 feet but is about 20,000 feet in figures 4(b), 4(c), and 4(d). For each of these maneuvers the Δp_0 and t plots show two separate sets of experimental data which indicate that two complete, separate N-waves were recorded. The theory predicts correctly the observed number of waves over the microphone array and generally gives the elapsed times within a few seconds of those measured. The theoretical elapsed times are usually somewhat less than those observed.

It should be pointed out that, depending upon the observer location and the flight conditions of this pushover-dive-pullout maneuver, from one to three complete N-waves could be observed. (See figs. 18 and 19 from ref. 6.)

The Δp_0 plots show that as long as the ground pattern near the microphone array does not exhibit a cusp or focus, the overpressure calculations either give a good mean value of the measured pressures in the strongest wave or occasionally tend to overestimate the strength. The measured overpressures in the weaker waves are also usually somewhat less than those calculated.

Longitudinal Acceleration at Constant Altitude

Figure 5 shows the results for four linear accelerations at constant altitude. The flight conditions and layout of these maneuvers for figure 5 are shown in figure 2(a). The distance along the ground from the center of the array to the point at which $M = 1$ was about 70,000 feet for figures 5(a), 5(b), and 5(c), and was only about 50,000 feet for figure 5(d). In addition, for the case shown in figure 5(d), the aircraft Mach number over the center of the array was only 1.14. For these maneuvers it was found that the aircraft position could be accurately represented by an analytical expression of the form $x = A + Bt + Ct^2$ where t is airplane flight time. The constants A,B,C were determined from the radar tracking data by the method of least squares. The aircraft velocity and acceleration were then derived from this expression. The aircraft Mach number obtained from this equation and measured weather data agreed with reports made by the pilot during the flights.

Figure 5 shows that one or two complete N-waves were observed at the microphone locations and in each case the theory predicts the correct number of waves.

In figures 5(a) and 5(b) the tone signal is missing from the experimental records so that the zero reference for the measured elapsed times is not known. However, the theory and experiment are in good agreement in regard to the time increment between successive waves. In figure 5(c), the theory is seen to give good estimates of the elapsed times. The calculated overpressures again give a good mean value of the pressures measured in the strongest wave and tend to overestimate the pressure in the weaker wave.

Figure 5(d) shows a clear case of a superbomb resulting from the acceleration. (The term "superboom" is used to refer to a localized increase in overpressure whose magnitude is considerably larger than that which would be expected from level flight at the same altitude and Mach number.) The microphone located at $x = -11,400$ feet recorded no boom; the one at $x = -3,200$ feet recorded only a single N-wave of approximately twice the overpressure normally expected for this altitude; all other microphones recorded two separate N-waves. The experimental data indicate that the cusp at which the two waves coalesce touched the ground in the neighborhood of $x = -3,200$ feet. The theory also predicts a cusp, but at a distance of about 2 miles farther down the flight track than observed. The pressure calculations, which are based on acoustic theory, are no longer reliable near the cusp. As expected, they indicate a considerable increase in the overpressure at the cusp but do not give meaningful quantitative information.

Pullup-Climb-Pushover Maneuver

Figure 6 shows a plan view and a profile view of a pullup-climb-pushover maneuver which was not part of the regular flight-test program but which was also carried out in the vicinity of Rogers Dry Lake at Edwards Air Force Base. The flight path was essentially confined to a vertical plane and had the approximate dimensions shown in figure 6(a). Radar tracking and weather information were obtained, but ground pressure measurements were recorded by only one microphone which was slightly off the flight track as indicated in figure 6(b). The measured pressure signature is shown in figure 6(c). Note that in this case the second N-wave to arrive had the highest overpressure. Theory predicted multiple booms and normal overpressures in the hatched region in the figure and in a similar symmetrically situated region on the other side of the flight track. The shock waves which fall within these two areas originate from the push-over and level-out portion of the maneuver. As in the case of the superbomb in figure 5(d), the calculated position of the double boom is somewhat farther down the flight track than indicated by experiment.

Circular-Turn Maneuvers at Constant Altitude

Figure 7 presents the results for four 90° circular turns and figure 8 shows the results for a 360° turn. A plan view of these maneuvers is shown in figure 2(d). In figure 7(a) the zero reference for the measured elapsed time

is missing from the experimental records so that only the number of waves and the difference in the elapsed times can be compared. The altitude for all flights was between 32,000 and 34,000 feet. The radii of the turns varied between 30,000 and 50,000 feet and the Mach number varied between 1.4 and 1.5. This is equivalent to a centripetal acceleration between 1.5g and 2.5g. The distance b along the X axis from the origin to the point at which the aircraft made its second pass over the X axis was varied between 0 and 30,000 feet. (See fig. 2(d).)

Except the flight in figure 7(d), from 2 to 3 complete N-waves were observed. The dotted lines through the experimental data points in figures 7(b) and 8 have been inserted in an attempt to render plausible the interpretation that one of the N-waves observed separated as it propagated along the microphone array.

Since the turn maneuvers are not confined to a vertical plane, the ground pattern is not symmetric on either side of the flight track but is definitely two dimensional in nature. This asymmetry makes a comparison of the theory and experiment somewhat more difficult for these cases. The preceding examples would indicate that the calculations should give essentially the correct pattern but that it will be displaced from the measured position laterally as well as longitudinally.

The calculated curves for figures 7(b) and 8 indicate a cusp crossing the microphone array. The Δp_0 curves predict a corresponding increase in the overpressures at the cusp. The experiment shows a similar phenomenon but suggests that the cusp occurred off the microphone array and initially consisted of a single shock wave which eventually separated into two distinct waves. There is no indication that the predicted pressure buildups occurred along the microphone array. However, such increases could have taken place near the cusps at some lateral distance from the array and therefore would not show up on the experimental records. In figure 7(d) both theory and experiment indicate a localized pressure buildup which apparently results from a focus.

Figures 7 and 8 again show that the theory used gives the correct number of booms observed near the microphone array and provides reasonable estimates of the elapsed times and ground overpressures.

FRIEDMAN SONIC BOOM COMPUTER PROGRAM

A method for computing the location and strength of the ground shock pattern which attempts to take into account some of the nonlinear effects of shock propagation and which allows for arbitrary variations in pressure, temperature, and winds with altitude is given in reference 9. At present this method is applicable to maneuvers in a vertical plane, but not in a horizontal plane. The procedure is based upon ray tracing and gives the ground locus of the shock waves produced at a given point on the flight path. These shock ground loci must then be suitably combined to obtain the ground shock pattern at a given instant of time.

Figures 9 and 10 show a comparison of calculations based upon the method of reference 9 for maneuver cases 2 and 8 with the experimental measurements. Figure 9 (case 2, table I) is for the supersonic-dive maneuver shown in figure 4(b). Figure 10 (case 8) is for the linear acceleration shown in figure 5(d). The actual temperature, pressure, and wind profiles measured prior to these flights were used in the calculations. The same part of the flight path was used in these calculations as was used in figures 4(b) and 5(d). It can be seen from figure 9 that the method of reference 9 predicts the amplitude and elapsed time of the initial disturbance with about the same accuracy as the method of the present paper. The presence of the second disturbance was not predicted. There is some indication that insufficient tracking data were available for the proper application of the method of reference 9 for the prediction of this second disturbance.

In figure 10 the predicted location of the superbomb is about 2 miles farther down the track than is measured; this result is very similar to that presented in figure 5(d). Neither Friedman's method nor the method used elsewhere in this paper can predict quantitatively the overpressure in the superbomb.

CONCLUDING REMARKS

The comparison between acoustic theory and experiment which is presented in this paper indicates that the method used is capable of predicting the essential features of the ground shock patterns of aircraft in maneuvers at altitudes below 30,000 to 40,000 feet at least when the sound speed gradient is nearly linear. In particular, the theory predicts the correct number of N-waves which will occur in the vicinity of a given ground area and gives reasonable estimates of the arrival times. In general, the calculated elapsed times are a few seconds less than those measured. The results suggest that the location of superbomb phenomena can be predicted within plus or minus 2 to 3 miles, provided accurate aircraft position information and weather data are available. The calculated overpressures either agree well with measurements or give a slight overestimate in those ground areas which are removed from cusps and do not experience superbomb phenomena.

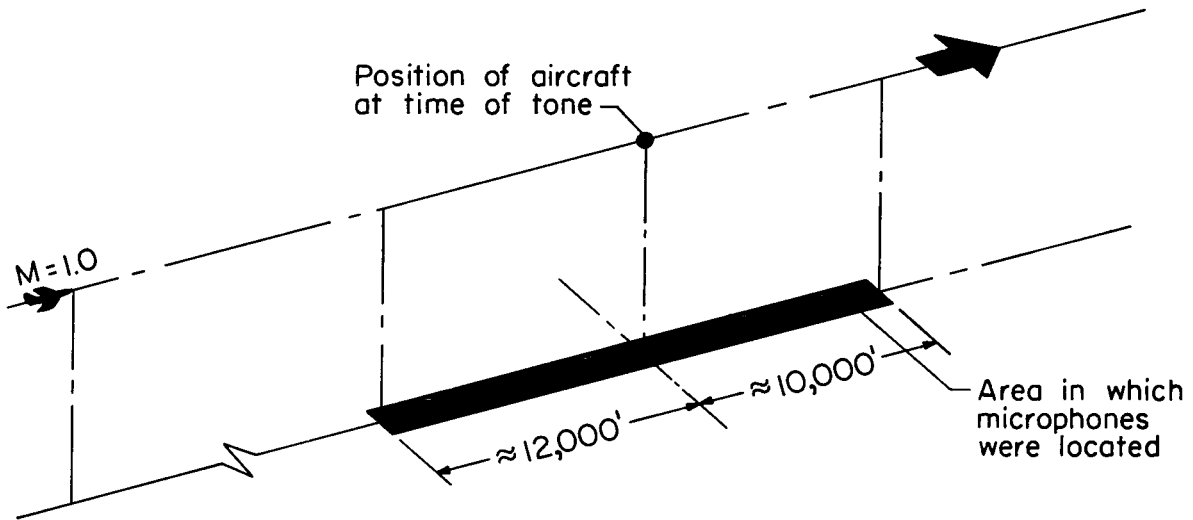
Langley Research Center,
National Aeronautics and Space Administration,
Langley Station, Hampton, Va., January 14, 1965.

REFERENCES

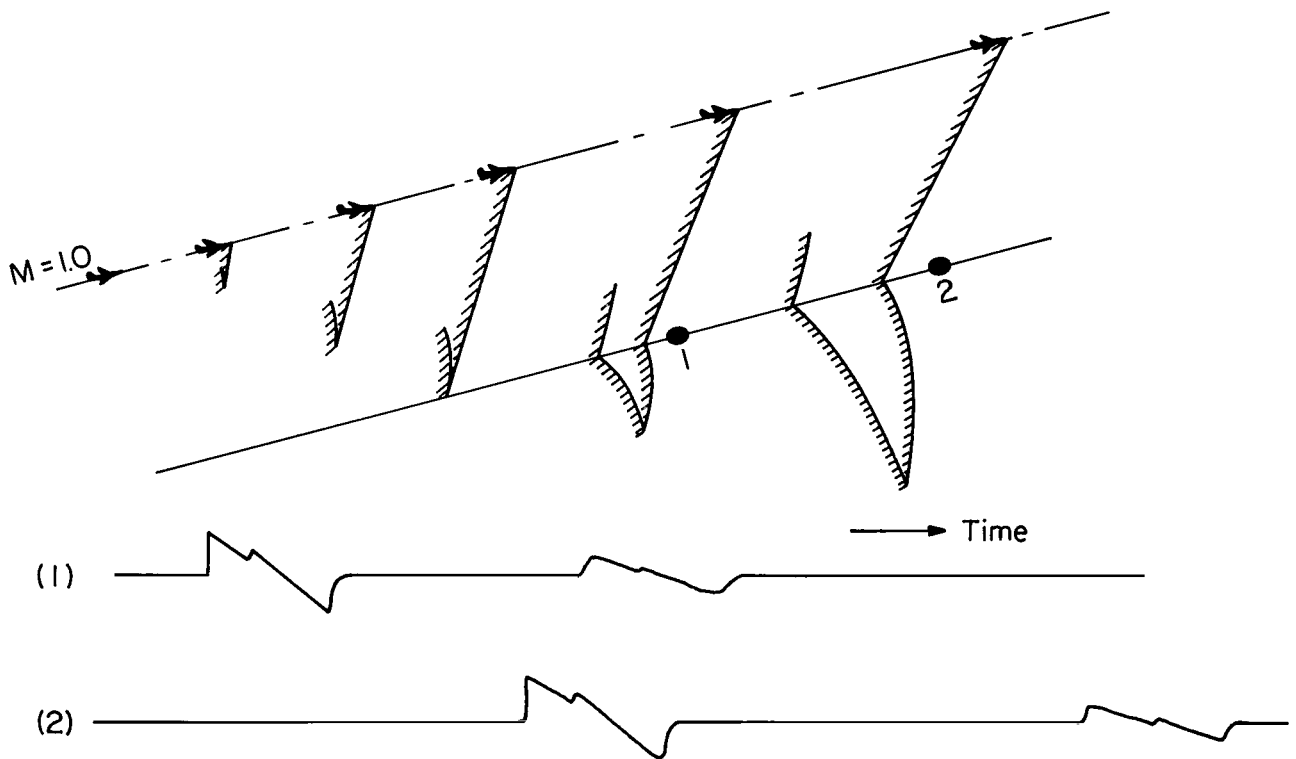
1. Lilley, G. M.; Westley, R.; Yates, A. H.; and Busing, J. R.: On Some Aspects of the Noise Propagation From Supersonic Aircraft. Rep. No. 71, The College of Aeronautics, Cranfield (British), Feb. 1953.
2. Rao, P. Sambasiva: Supersonic Bangs. Aeron. Quart., Vol. VII. Part 1, pt. I, Feb. 1956, pp. 21-44. Part 2, pt. II, May 1956, pp. 135-155.
3. Randall, D. G.: Methods for Estimating Distributions and Intensities of Sonic Bangs. R. & M. No. 3113, British A.R.C., 1959.
4. Lansing, Donald L.: Some Effects of Flight Path Upon the Distribution of Sonic Booms. Proc. Symposium on Atmospheric Acoustic Propagation, vol. I. June 14-16, 1961, pp. 24-43. (Sponsored by U.S. Army Signal Missile Support Agency and Texas Western College.)
5. Barger, Raymond L.: Some Effects of Flight Path and Atmospheric Variations on the Boom Propagated From Supersonic Aircraft. NASA TR R-191, 1964.
6. Lansing, Donald L.: Application of Acoustic Theory to Prediction of Sonic-Boom Ground Patterns From Maneuvering Aircraft. NASA TN D-1860, 1964.
7. Hubbard, Harvey H.; Maglieri, Domenic J.; Huckel, Vera; and Hilton, David A. (With appendix by Harry W. Carlson): Ground Measurements of Sonic-Boom Pressures for the Altitude Range of 10,000 to 75,000 Feet. NASA TR R-198, 1964. (Supersedes NASA TM X-633.)
8. Maglieri, Domenic J.; and Lansing, Donald L.: Sonic Booms From Aircraft in Maneuvers. NASA TN D-2370, 1964.
9. Friedman, Manfred P.: A Description of a Computer Program for the Study of Atmospheric Effects on Sonic Booms. NASA CR-157, 1965.
10. Whitham, G. B.: The Flow Pattern of a Supersonic Projectile. Commun. Pure Appl. Math., vol. V, no. 3, Aug. 1952, pp. 301-348.
11. Anon: U.S. Standard Atmosphere, 1962. NASA, U.S. Air Force, and U.S. Weather Bureau, Dec. 1962.

TABLE I.- LOG OF SONIC-BOOM MANEUVER FLIGHTS

Type of maneuver	Case	Date	Time of day	Altitude, ft (mean sea level)	Mach number
Supersonic pushover-dive-pullout	1	9-14-61	0800	40,000 to 10,000	1.2 to 1.5
	2	10-5-61	0938	40,000 to 20,000	
	3	10-5-61	0946	40,000 to 20,000	
	4	10-5-61	0954	40,000 to 20,000	
Longitudinal acceleration at constant altitude	5	9-18-61	0840	14,600	1.0 to 1.16
	6	9-18-61	0846	14,200	1.0 to 1.17
	7	9-22-61	0933	14,200	1.0 to 1.17
	8	10-13-61	0954	13,800	1.0 to 1.14
Pullup-climb-pushover	9	5-27-63	0915	36,000 to 40,000	1.4
90° circular turn at constant altitude	10	9-21-61	0820	32,200	1.48
	11	9-21-61	0828	32,200	1.43
	12	9-21-61	0835	32,200	1.42
	13	10-3-61	0905	33,700	1.50
360° circular turn at constant altitude	14	10-3-61	0908	33,700	1.5

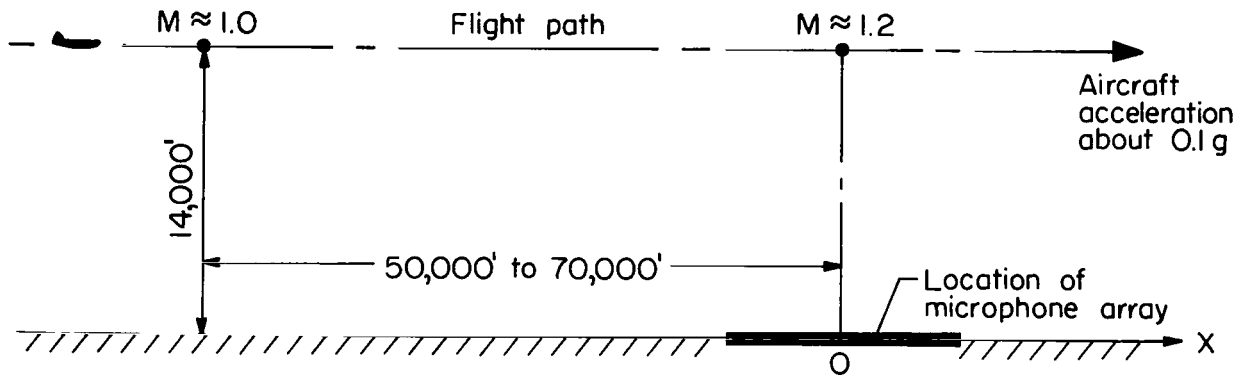


(a) Location of flight and ground track relative to ground microphone array.

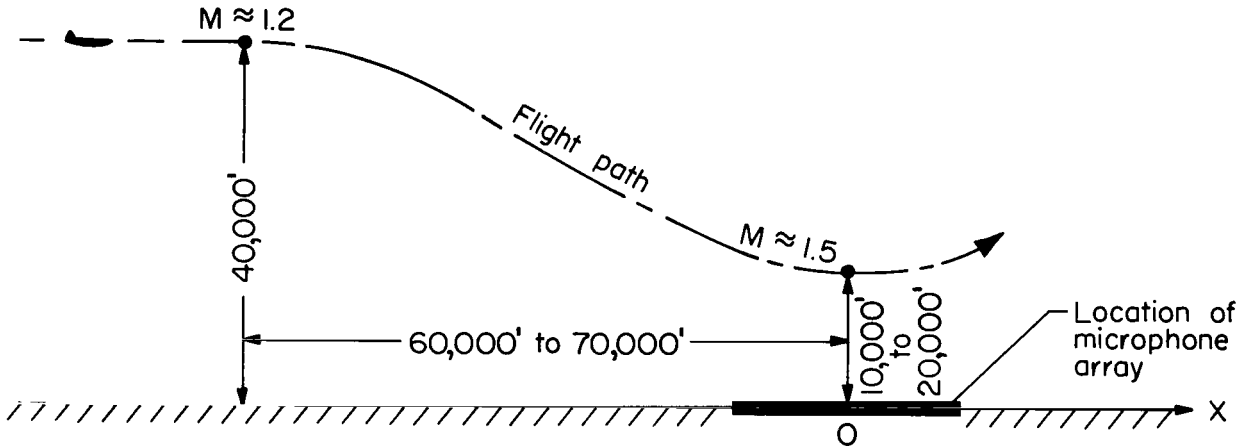


(b) Sketch of shock-wave formations and pressure signatures measured at points (1) and (2) for aircraft performing a longitudinal acceleration at a constant altitude.

Figure 1.- Sketch showing arrangement of test setup and type of measured data obtained.

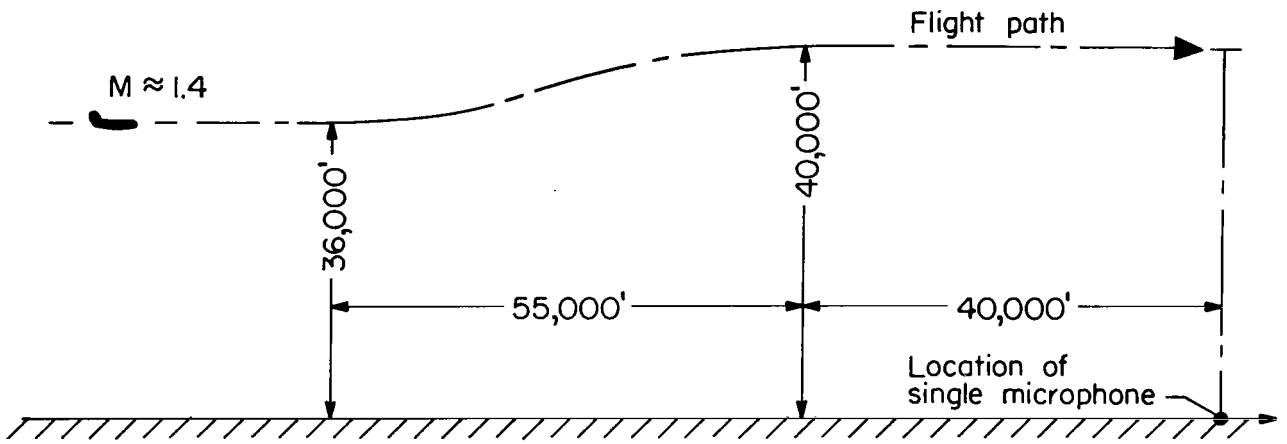


(a) Longitudinal acceleration (profile view).

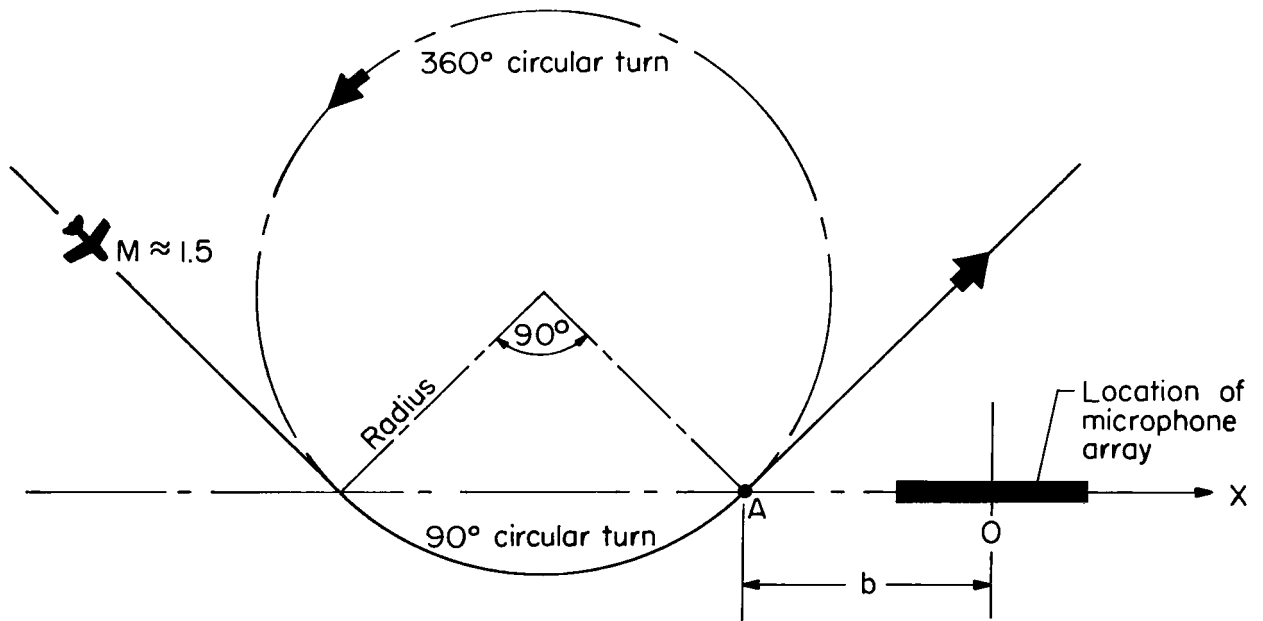


(b) Pushover-dive-pullout (profile view).

Figure 2.- Schematic illustrating types of maneuvers considered.



(c) Pullup-climb-pushover (profile view).



(d) Circular turns (planview).

Figure 2.- Concluded.

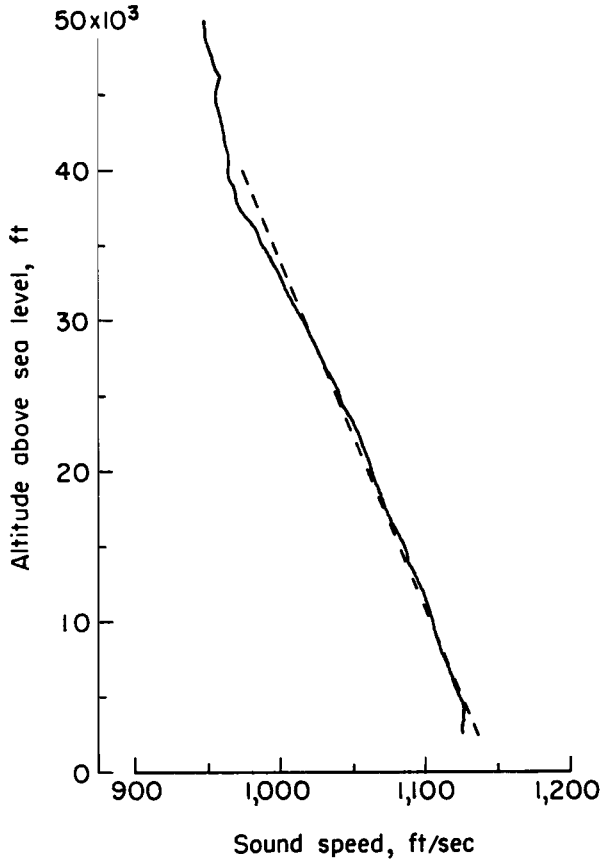
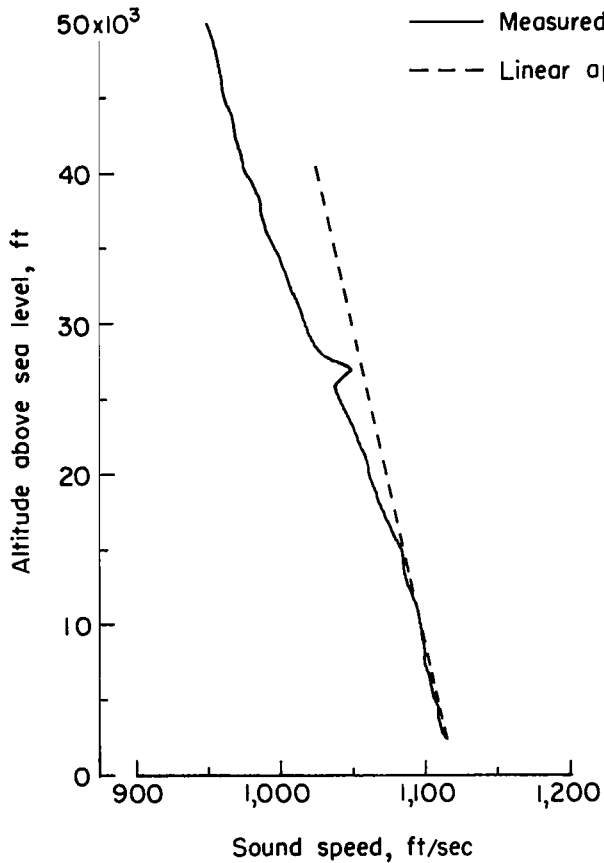
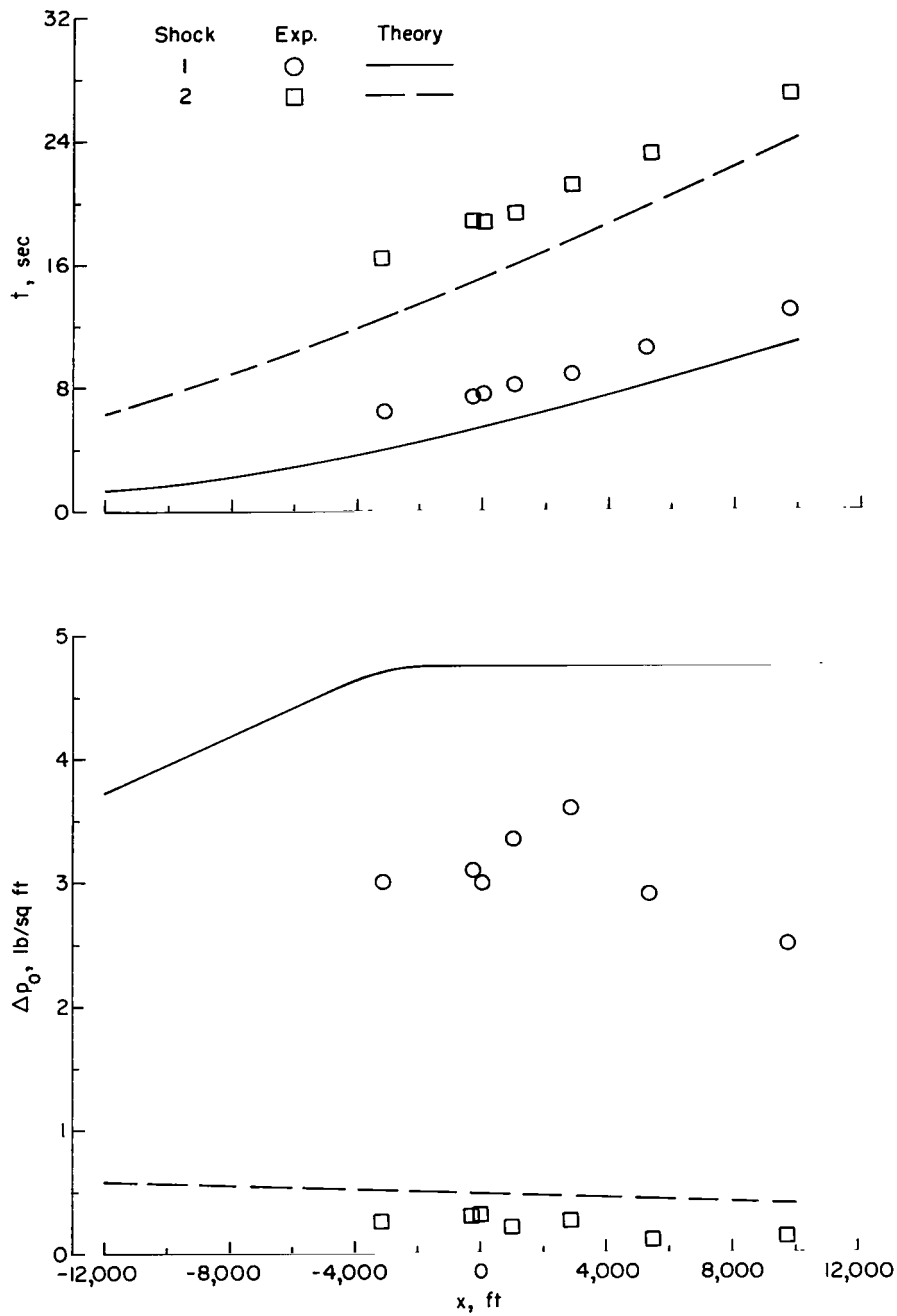
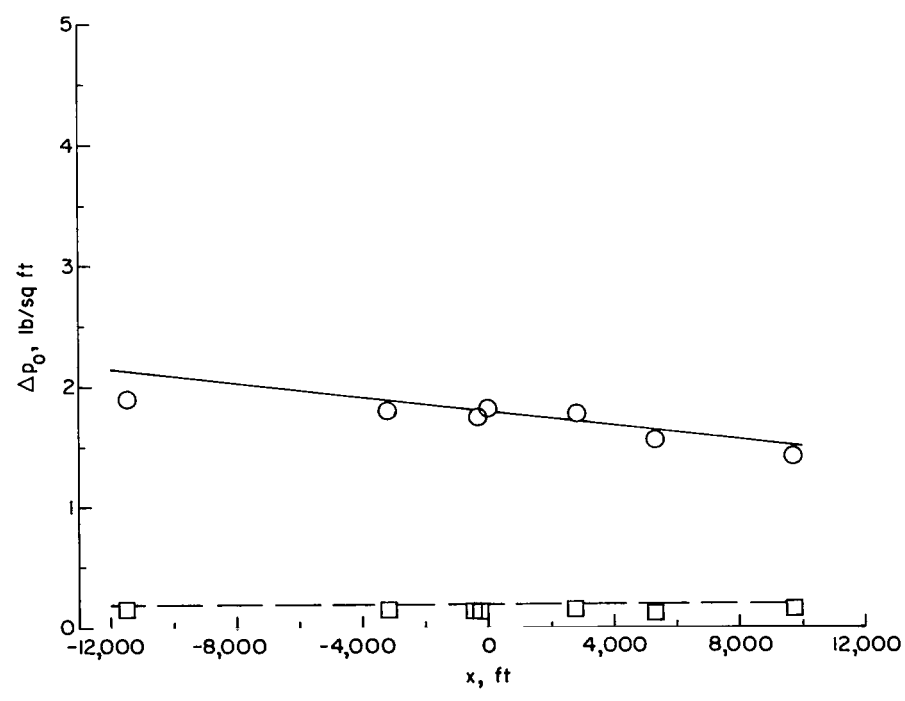
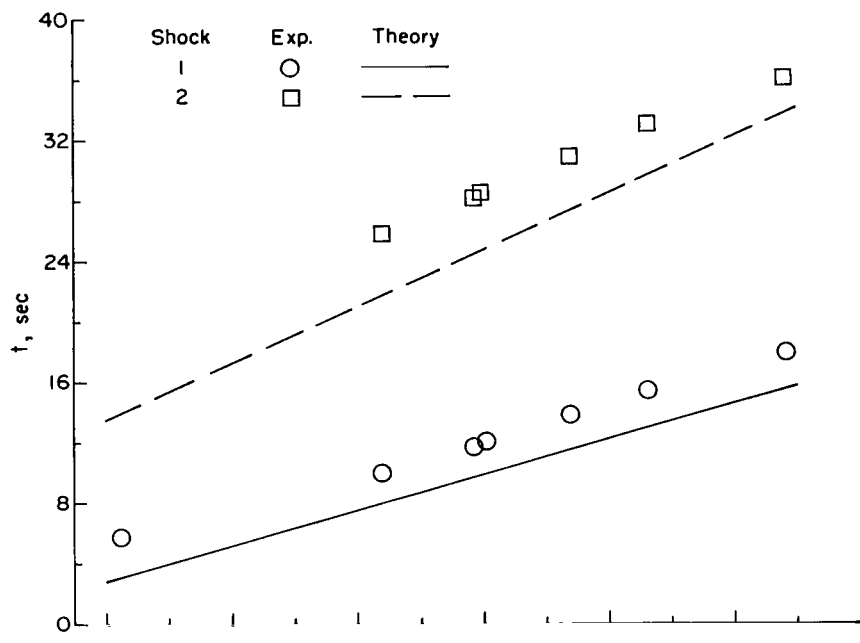


Figure 3.- Typical measured speeds of sound and linear approximation.



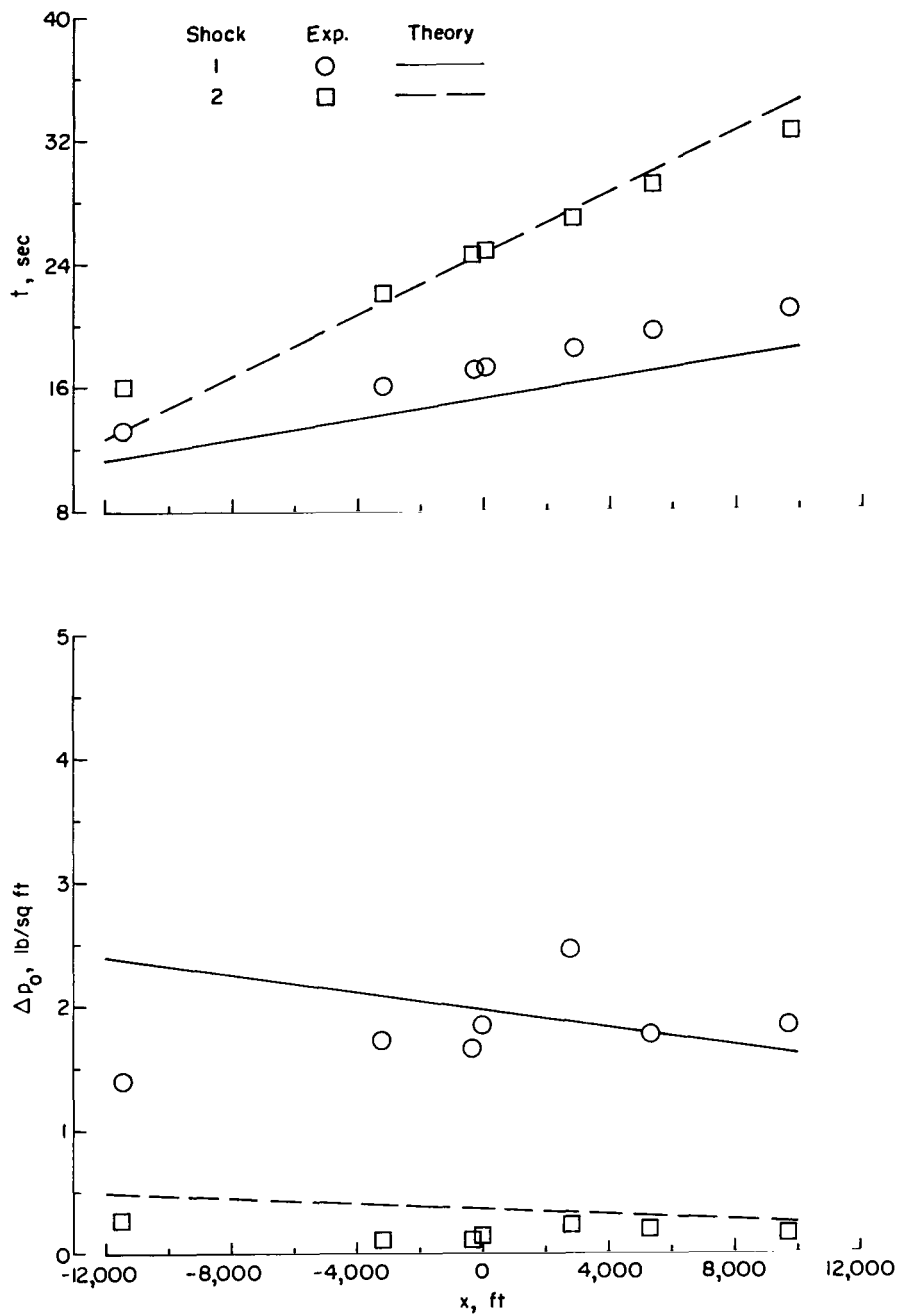
(a) Case 1.

Figure 4.- Comparison of calculated and measured elapsed times and overpressures for a pushover-dive-pullout maneuver.



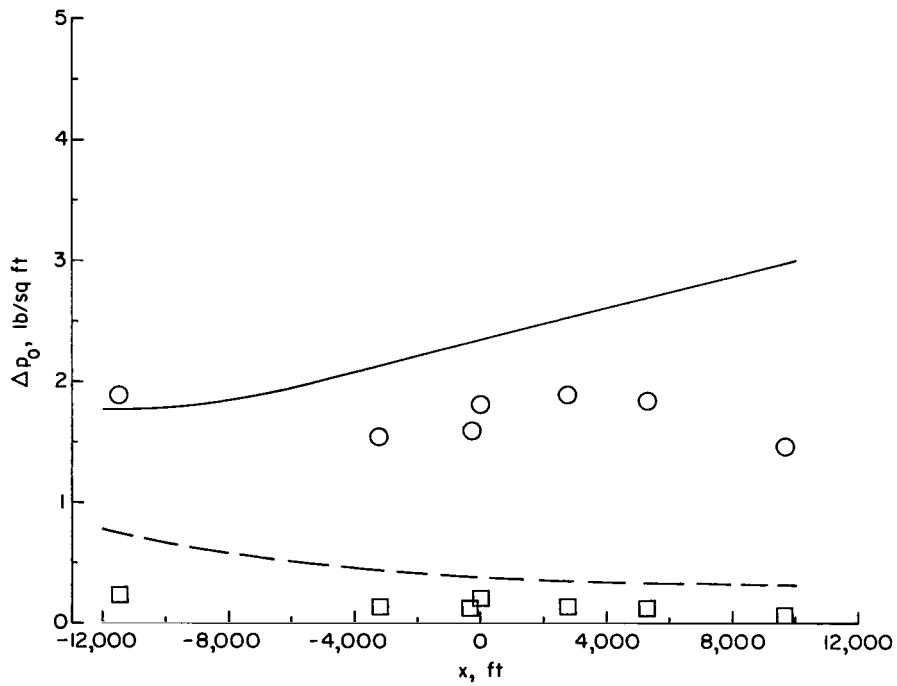
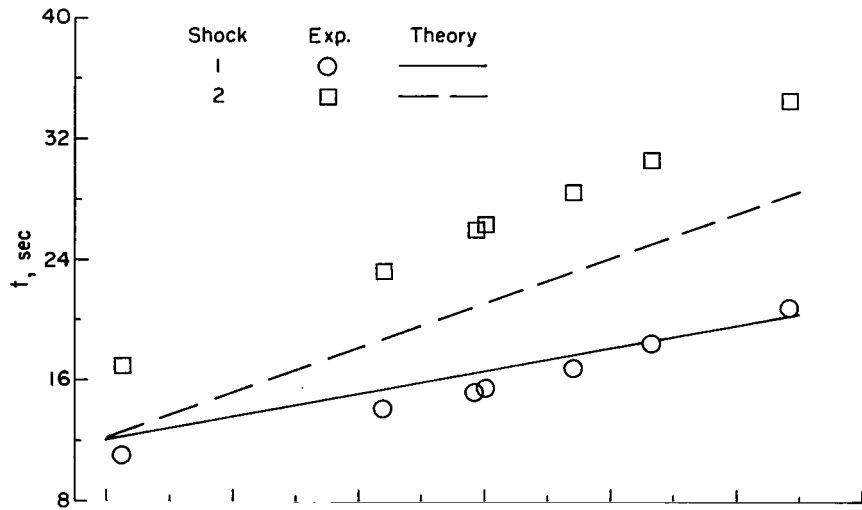
(b) Case 2.

Figure 4.- Continued.



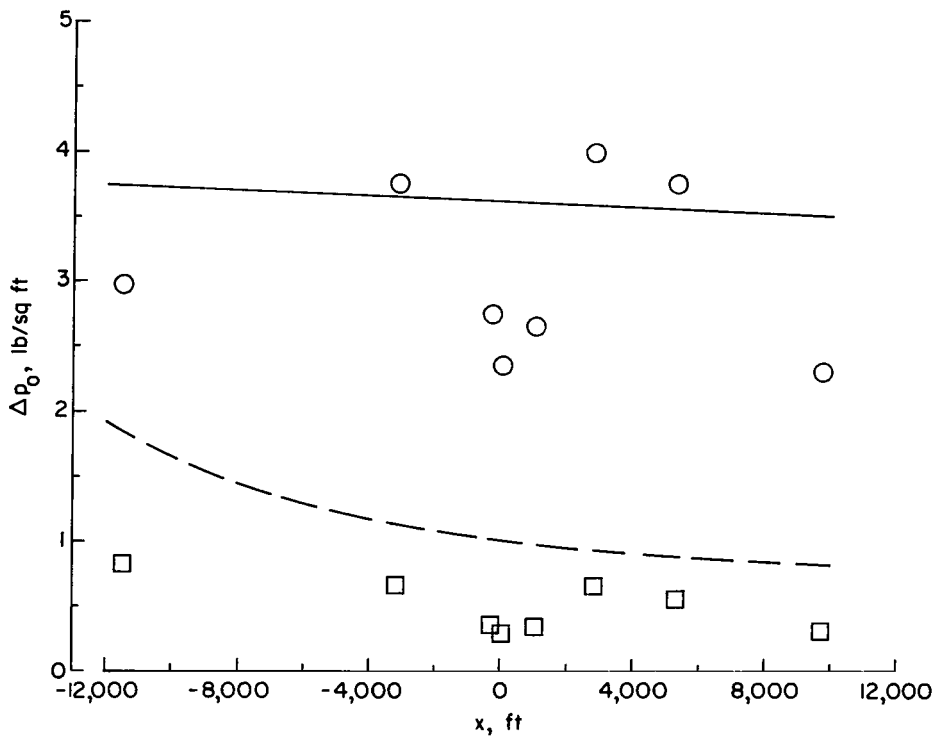
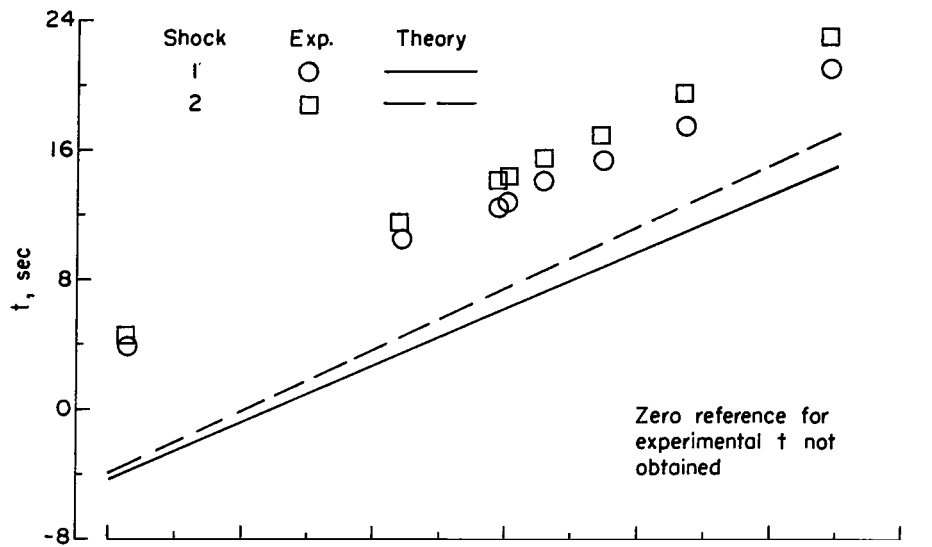
(c) Case 3.

Figure 4.- Continued.



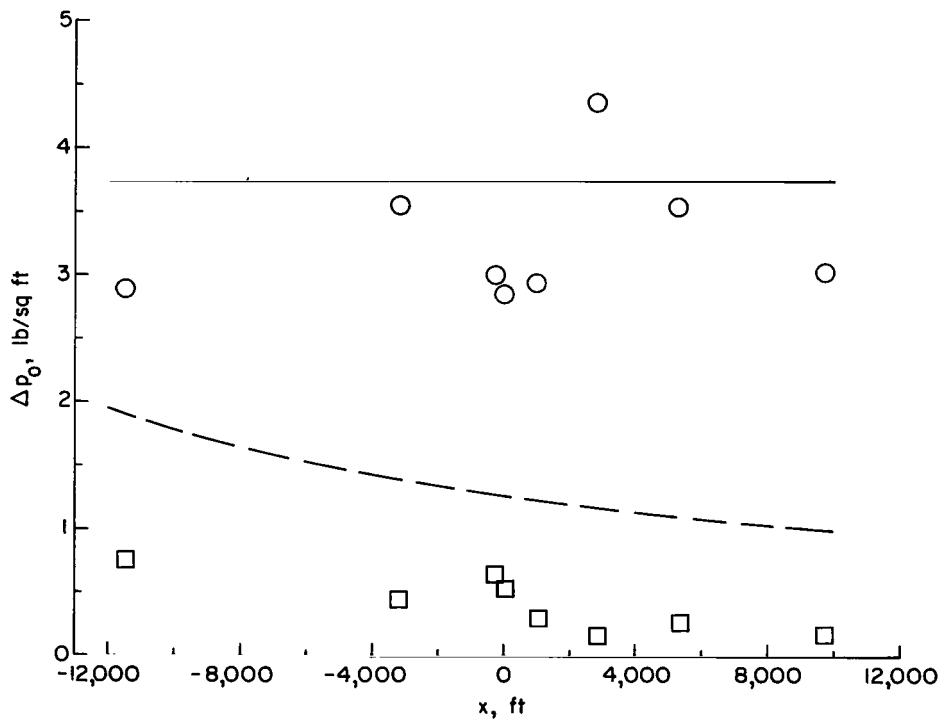
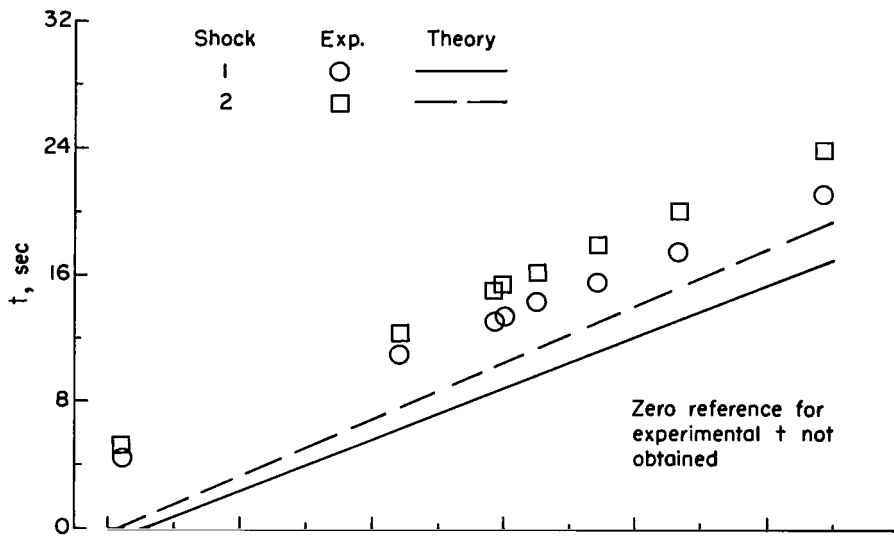
(d) Case 4.

Figure 4.- Concluded.



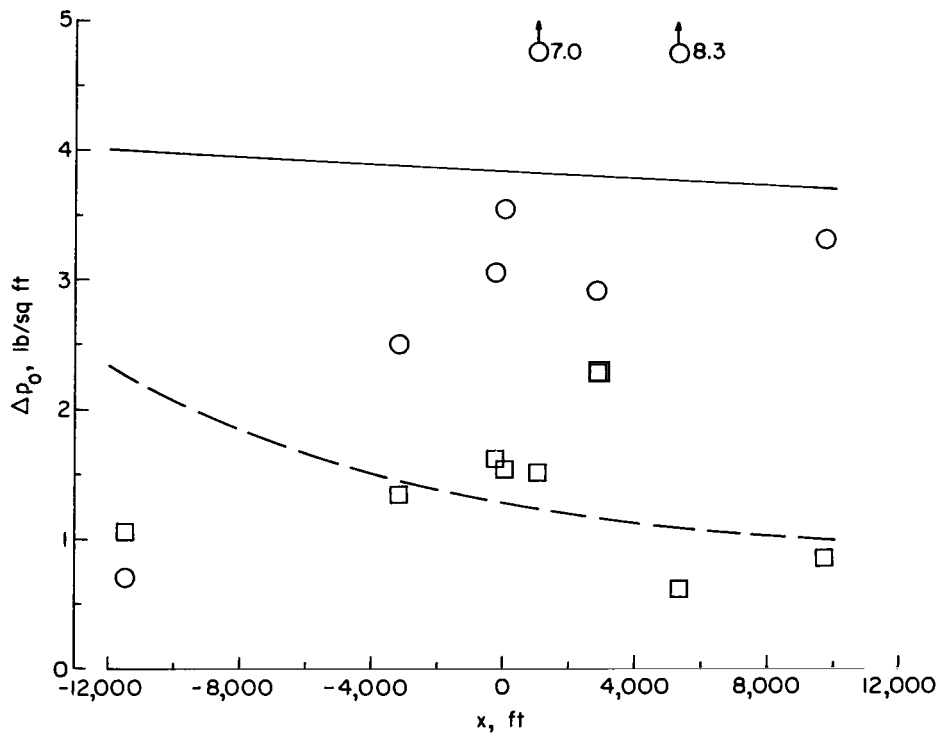
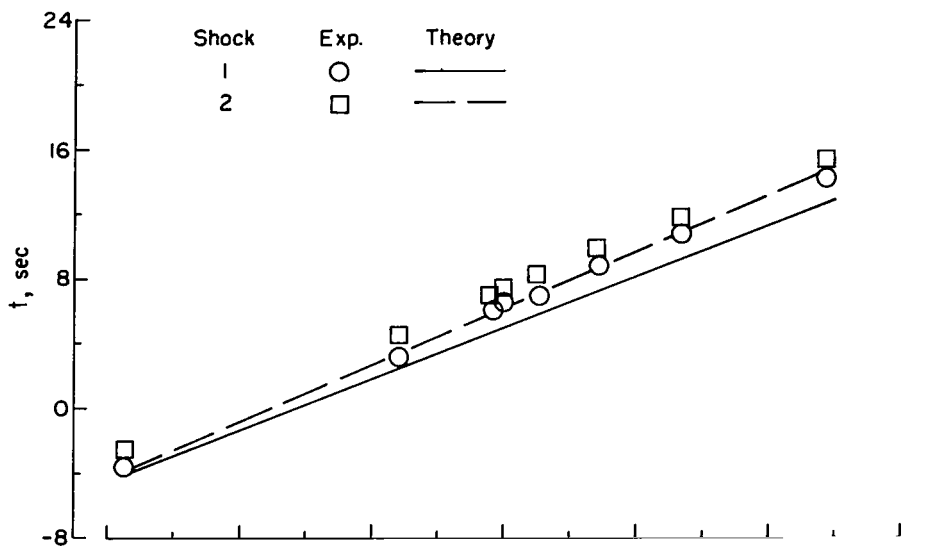
(a) Case 5.

Figure 5.- Comparison of calculated and measured elapsed times and overpressures for a longitudinal acceleration at constant altitude.



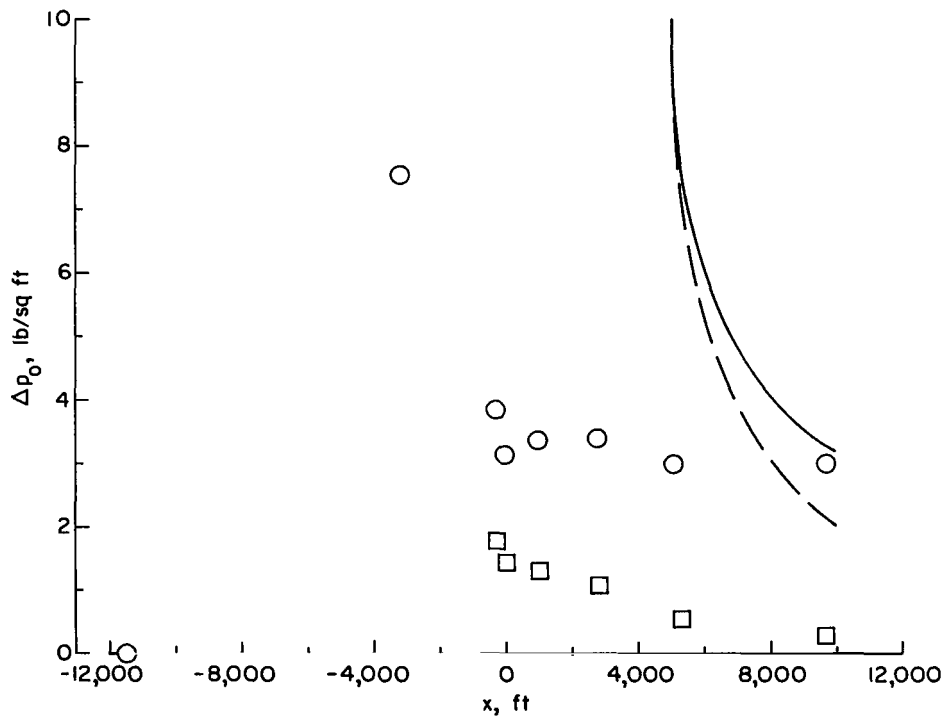
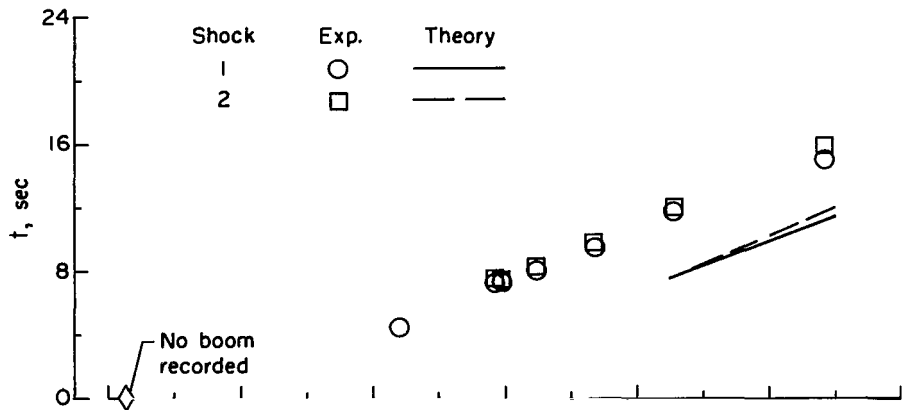
(b) Case 6.

Figure 5.- Continued.



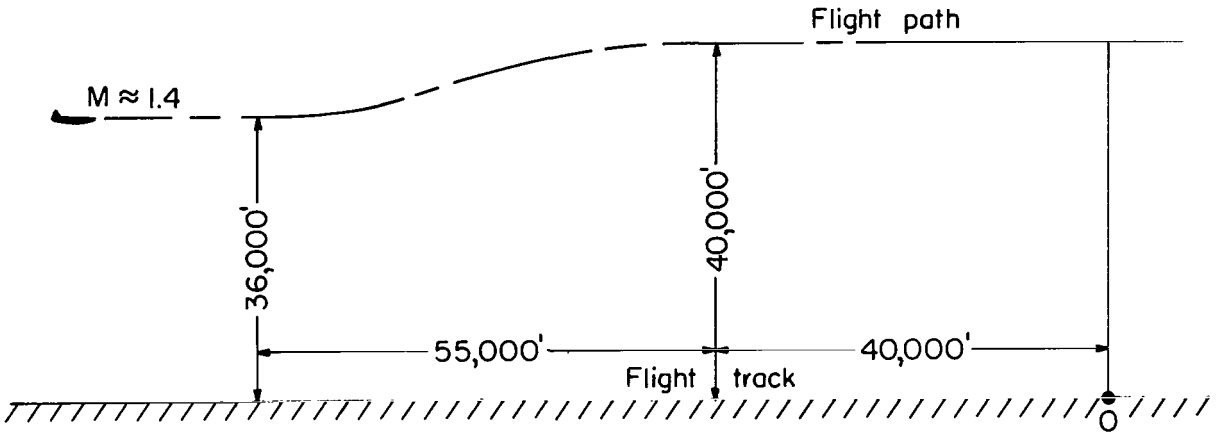
(c) Case 7.

Figure 5.- Continued.

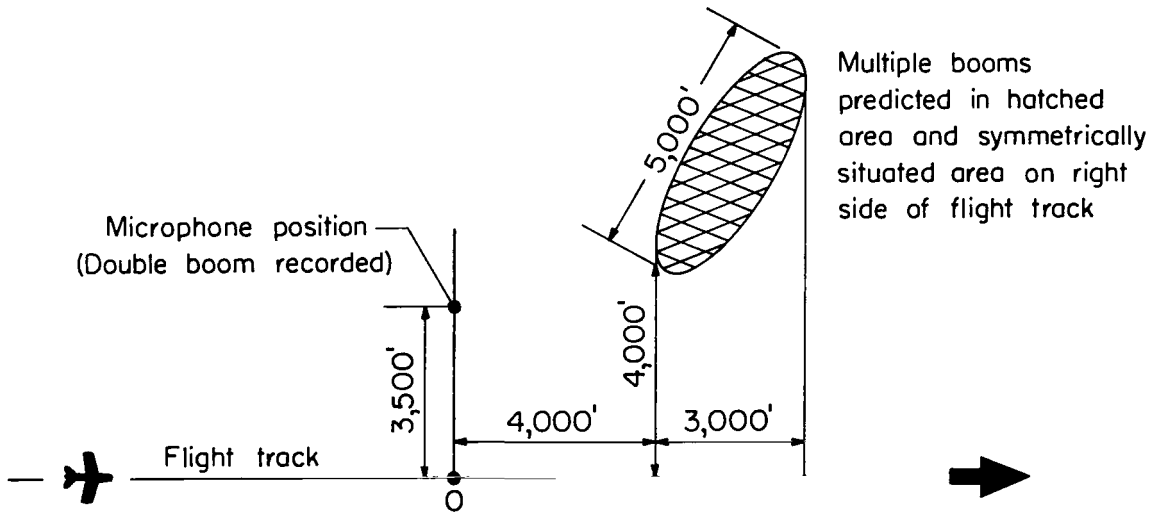


(d) Case 8.

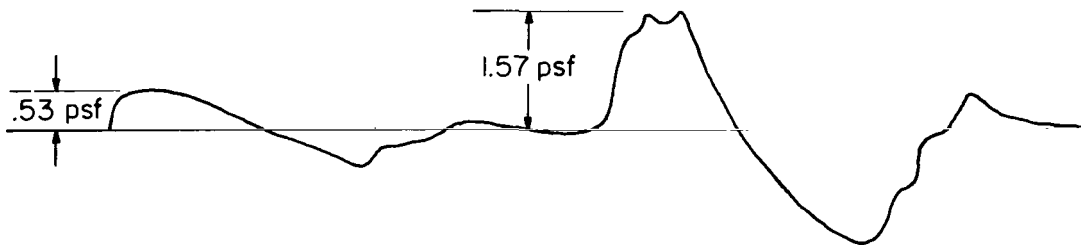
Figure 5.- Concluded.



(a) Profile view of pullup-climb-pushover maneuver.

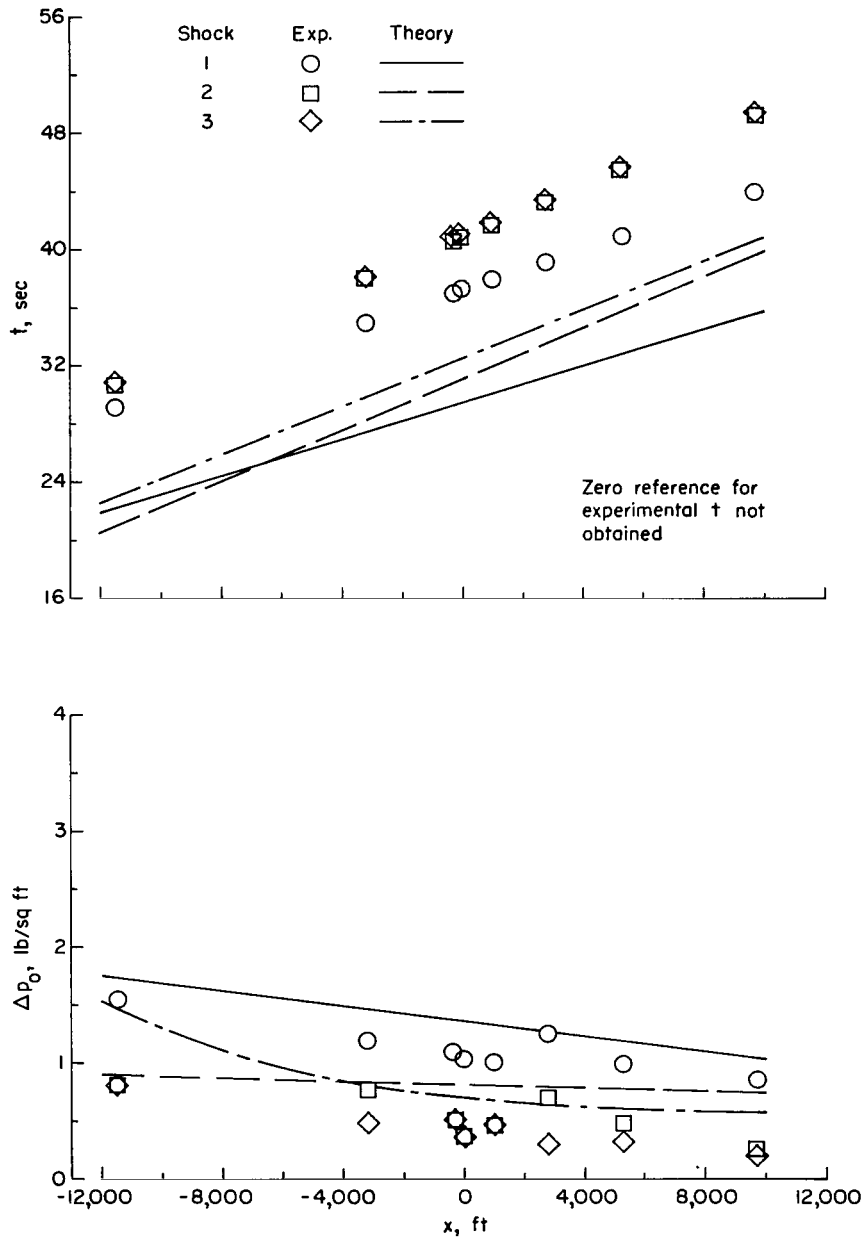


(b) Planview of pullup-climb-pushover maneuver.



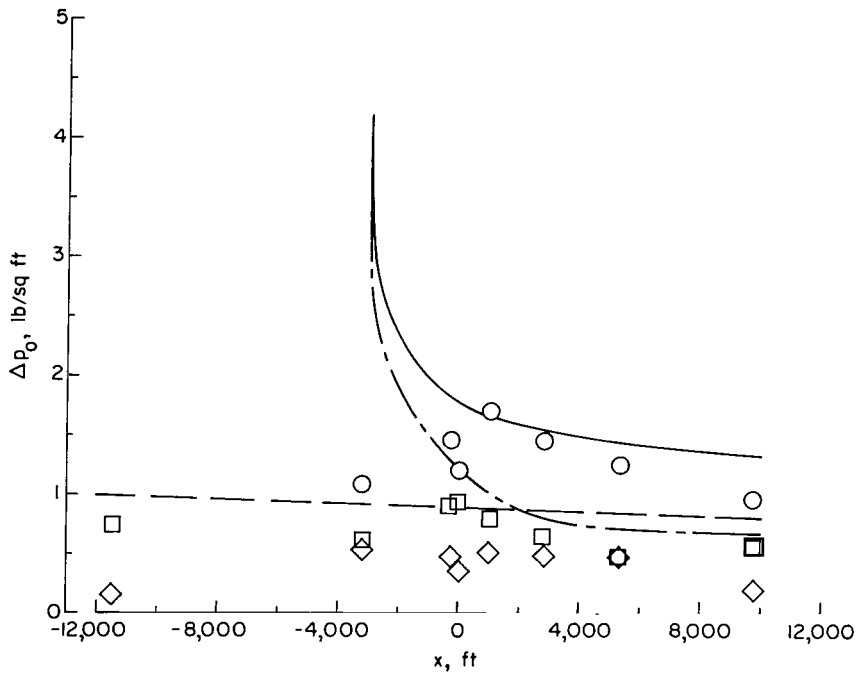
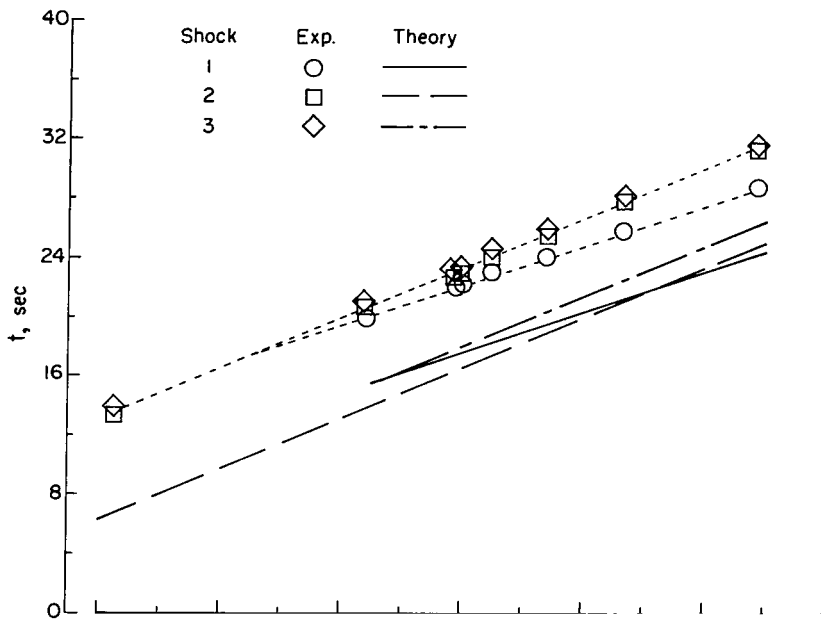
(c) Measured sonic-boom pressure signature.

Figure 6.- Flight track, ground microphone location, and areas of theoretical predicted multiple booms for a pullup-climb-pushover maneuver (case 9).



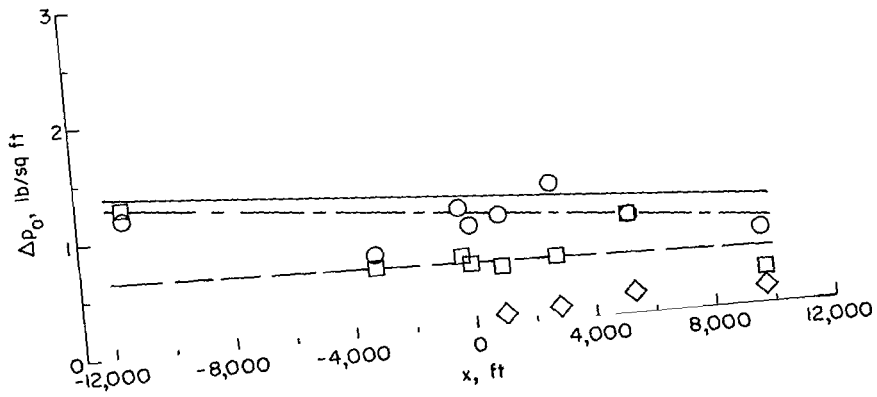
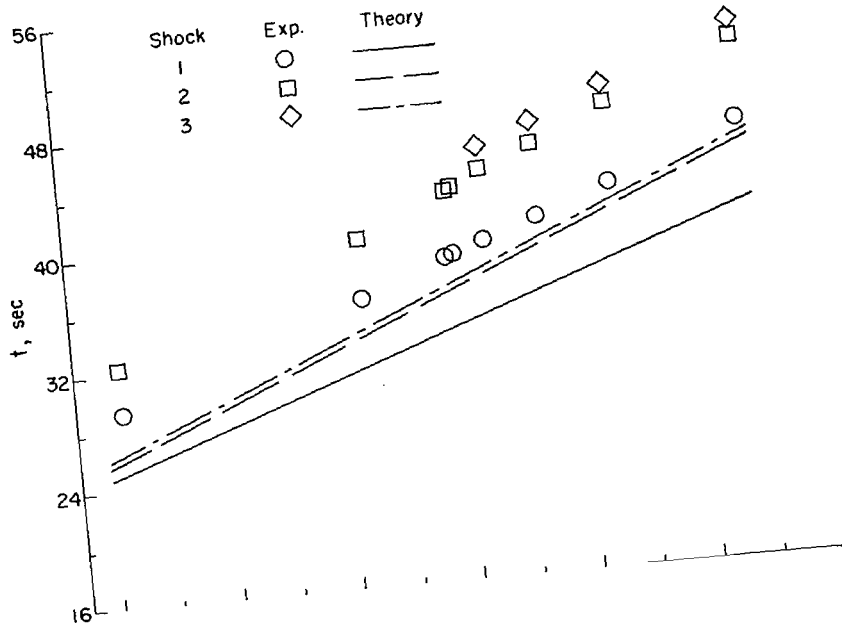
(a) Case 10.

Figure 7.- Comparison of calculated and measured elapsed times and overpressures for a 90° turn maneuver at constant altitude.

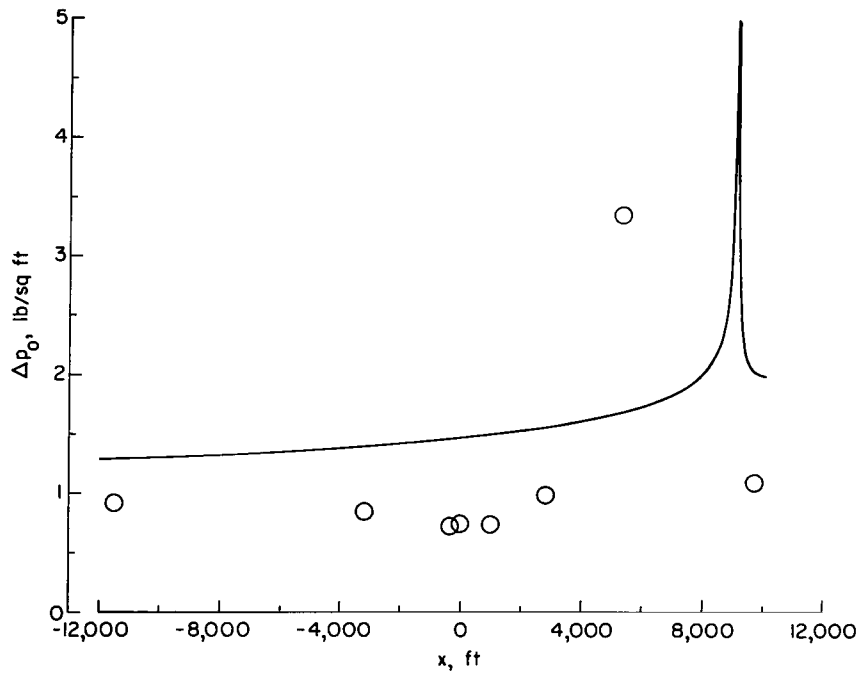
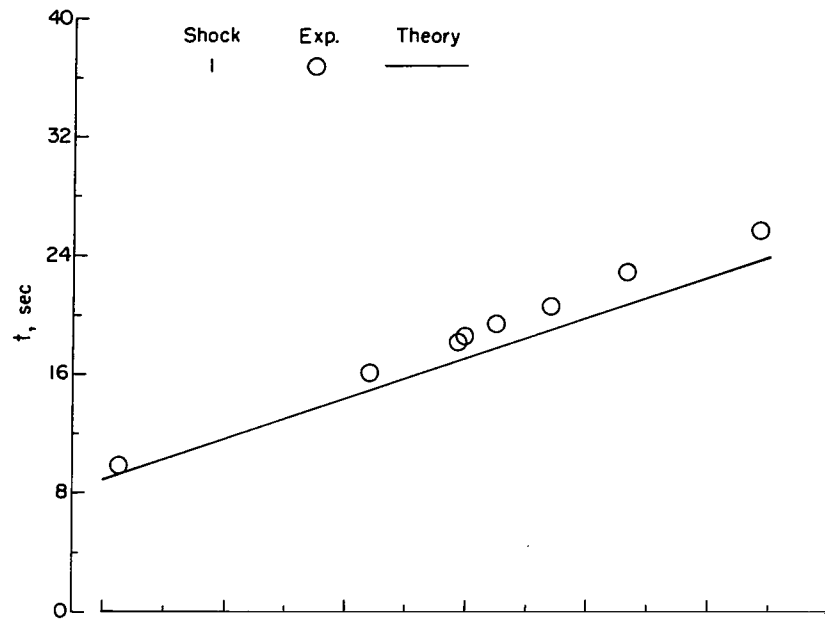


(b) Case 11.

Figure 7.- Continued.



(c) Case 12.
Figure 7.- Continued.



(d) Case 13.

Figure 7.- Concluded.

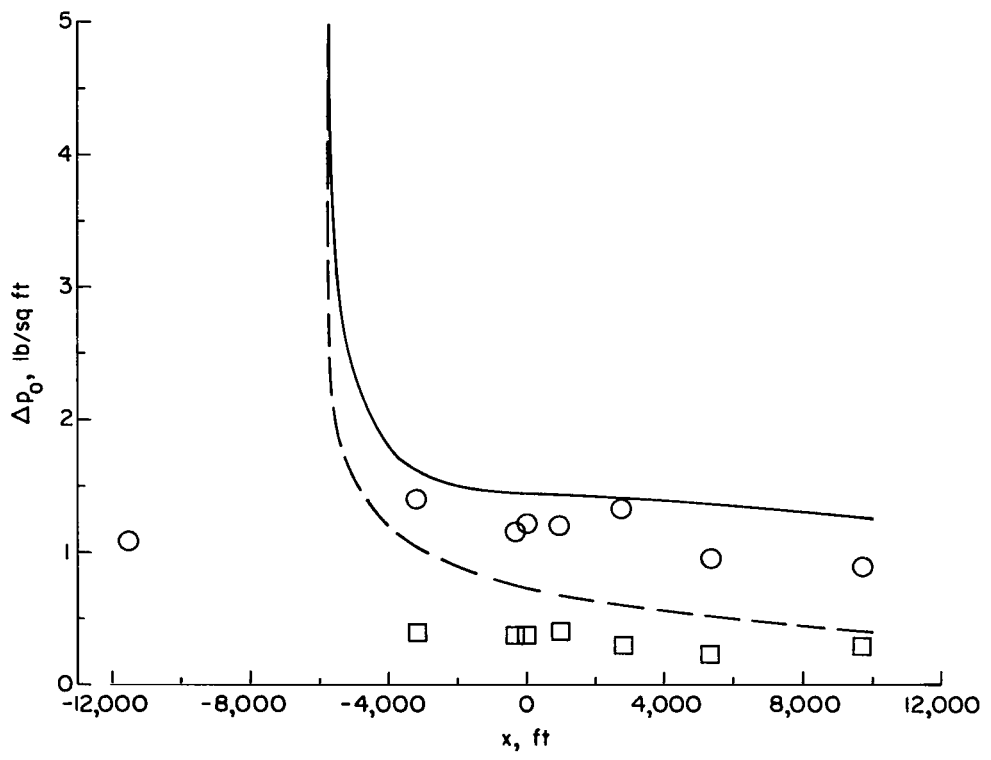
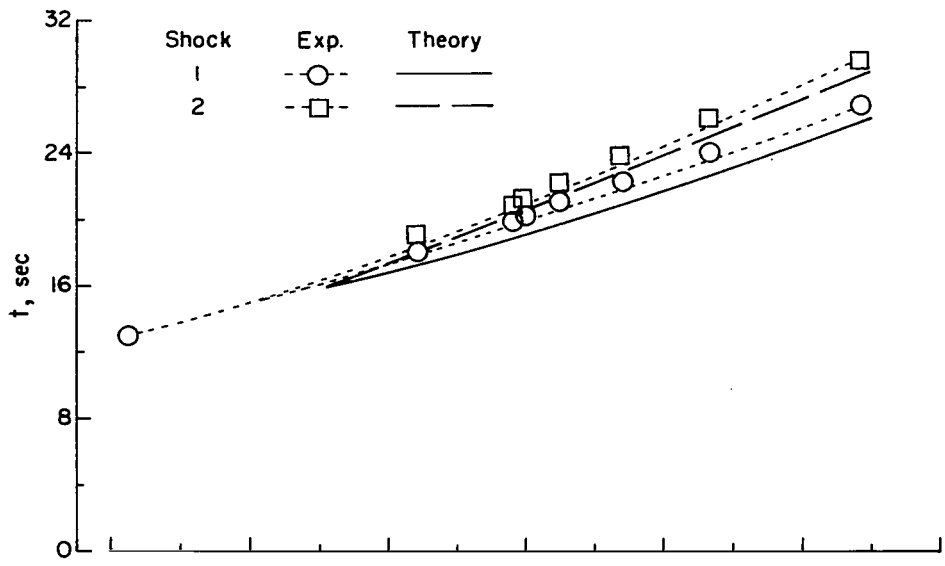


Figure 8.- Comparison of calculated and measured elapsed times and overpressures for a 360° turn maneuver at a constant altitude for case 14.

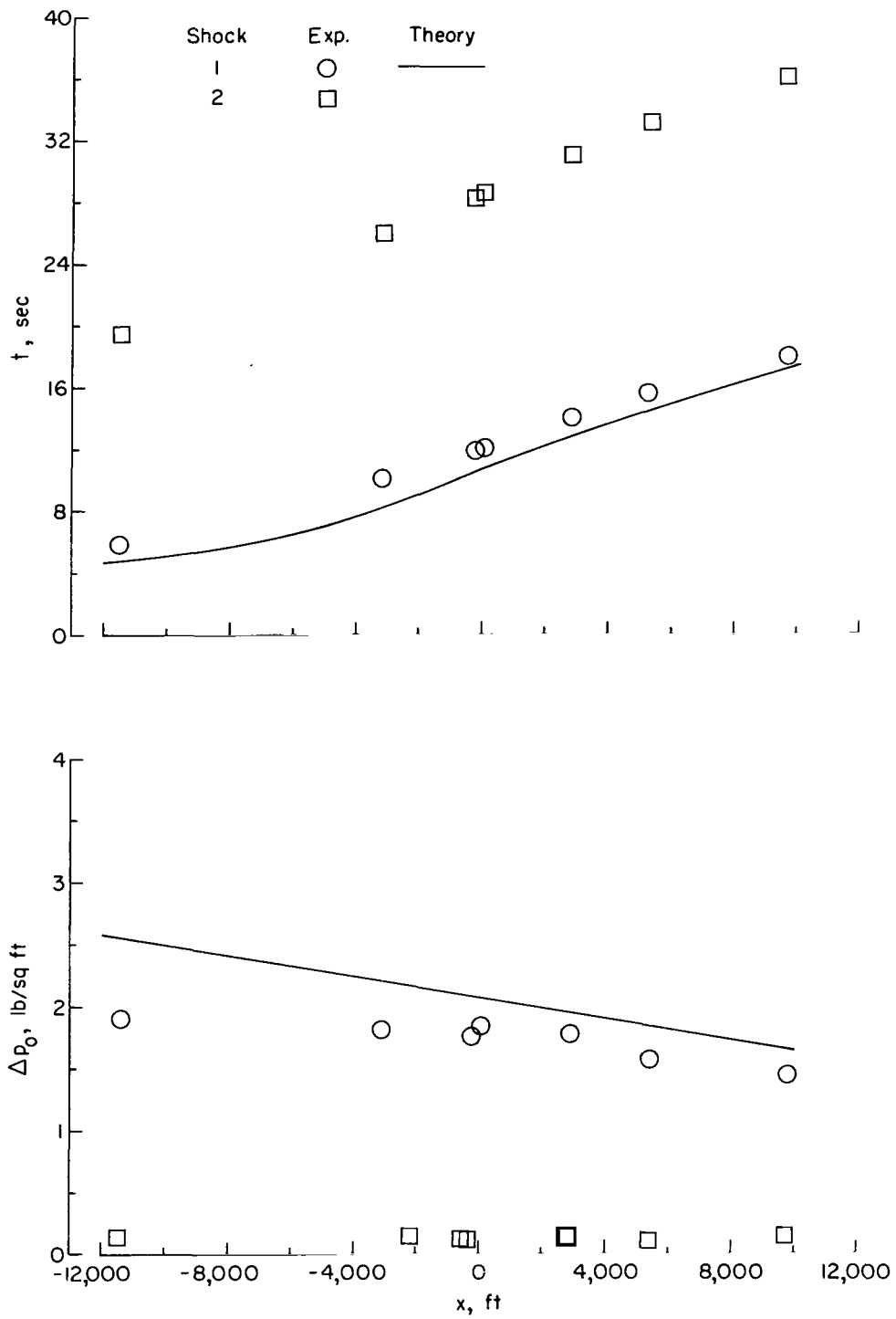


Figure 9.- Comparison of calculated and measured elapsed times and overpressures for a pushover-dive-pullout maneuver using method of reference 9 for case 2.

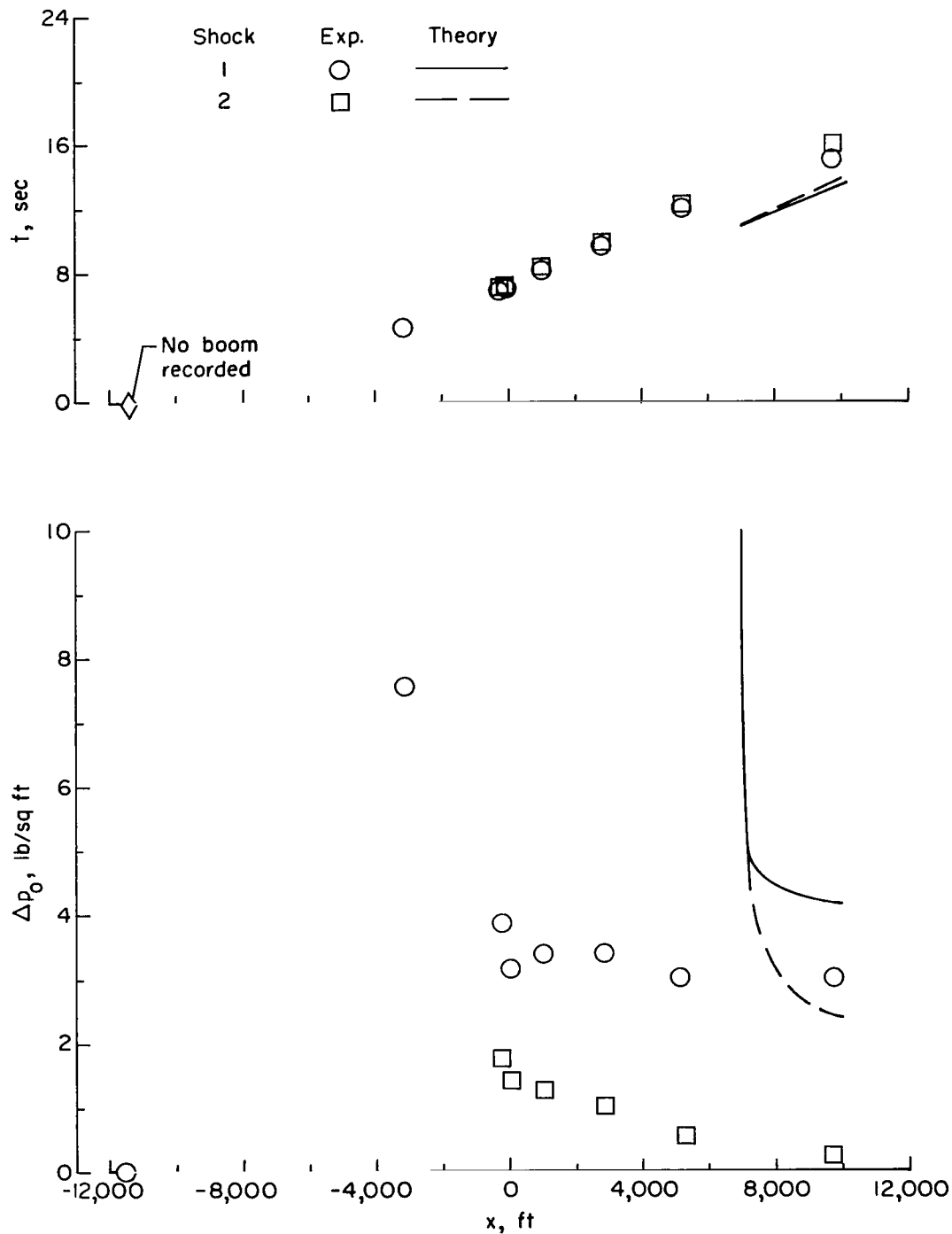


Figure 10.- Comparison of calculated and measured elapsed times and overpressures for a longitudinal acceleration at constant altitude using method of reference 9 for case 8.

2/22/85
5

"The aeronautical and space activities of the United States shall be conducted so as to contribute . . . to the expansion of human knowledge of phenomena in the atmosphere and space. The Administration shall provide for the widest practicable and appropriate dissemination of information concerning its activities and the results thereof."

—NATIONAL AERONAUTICS AND SPACE ACT OF 1958

NASA SCIENTIFIC AND TECHNICAL PUBLICATIONS

TECHNICAL REPORTS: Scientific and technical information considered important, complete, and a lasting contribution to existing knowledge.

TECHNICAL NOTES: Information less broad in scope but nevertheless of importance as a contribution to existing knowledge.

TECHNICAL MEMORANDUMS: Information receiving limited distribution because of preliminary data, security classification, or other reasons.

CONTRACTOR REPORTS: Technical information generated in connection with a NASA contract or grant and released under NASA auspices.

TECHNICAL TRANSLATIONS: Information published in a foreign language considered to merit NASA distribution in English.

TECHNICAL REPRINTS: Information derived from NASA activities and initially published in the form of journal articles.

SPECIAL PUBLICATIONS: Information derived from or of value to NASA activities but not necessarily reporting the results of individual NASA-programmed scientific efforts. Publications include conference proceedings, monographs, data compilations, handbooks, sourcebooks, and special bibliographies.

Details on the availability of these publications may be obtained from:

SCIENTIFIC AND TECHNICAL INFORMATION DIVISION
NATIONAL AERONAUTICS AND SPACE ADMINISTRATION
Washington, D.C. 20546